doi:10.1093/brain/awn243 *Brain* (2008), **131**, 3335–3347

Granulocyte-colony stimulating factor improves outcome in a mouse model of amyotrophic lateral sclerosis

Claudia Pitzer,[1] Carola Krüger,[1] Christian Plaas,[1] Friederike Kirsch,[1] Tanjew Dittgen,[1] Ralph Müller,[1] Rico Laage,[1] Stefan Kastner,[1] Stefanie Suess,[1] Robert Spoelgen,[1] Alexandre Henriques,[1] Hannelore Ehrenreich,[2] Wolf-Rüdiger Schäbitz,[3] Alfred Bach[1] and Armin Schneider[1]

[1]Sygnis Bioscience, Heidelberg, [2]Max-Planck Institute of Experimental Medicine, Göttingen and [3]Department of Neurology, University of Münster, Münster, Germany

Correspondence to: Dr Armin Schneider, Sygnis Bioscience, Im Neuenheimer Feld 515, 69120 Heidelberg, Germany
E-mail: schneider@sygnis.de

Amyotrophic lateral sclerosis (ALS) is a devastating neurodegenerative disease that results in progressive loss of motoneurons, motor weakness and death within 1–5 years after disease onset. Therapeutic options remain limited despite a substantial number of approaches that have been tested clinically. In particular, various neurotrophic factors have been investigated. Failure in these trials has been largely ascribed to problems of insufficient dosing or inability to cross the blood–brain barrier (BBB). We have recently uncovered the neurotrophic properties of the haematopoietic protein granulocyte-colony stimulating factor (G-CSF). The protein is clinically well tolerated and crosses the intact BBB. This study examined the potential role of G-CSF in motoneuron diseases. We investigated the expression of the G-CSF receptor in motoneurons and studied effects of G-CSF in a motoneuron cell line and in the SOD1 (G93A) transgenic mouse model. The neurotrophic growth factor was applied both by continuous subcutaneous delivery and CNS-targeted transgenic overexpression. This study shows that given at the stage of the disease where muscle denervation is already evident, G-CSF leads to significant improvement in motor performance, delays the onset of severe motor impairment and prolongs overall survival of SOD1 (G93A) tg mice. The G-CSF receptor is expressed by motoneurons and G-CSF protects cultured motoneuronal cells from apoptosis. In ALS mice, G-CSF increased survival of motoneurons and decreased muscular denervation atrophy. We conclude that G-CSF is a novel neurotrophic factor for motoneurons that is an attractive and feasible drug candidate for the treatment of ALS.

Keywords: ALS; growth factor; drug candidate; functional outcome; motoneuron survival

Abbreviations: ALS = amyotrophic lateral sclerosis; BBB = blood–brain barrier; CHAT = choline acetyltransferase; G-CSF = granulocyte-colony stimulating factor; SOD1 = superoxide dismutase 1

Received March 18, 2008. Revised July 17, 2008. Accepted September 8, 2008. Advance Access publication October 3, 2008

Introduction

Amyotrophic lateral sclerosis (ALS) is an incurable fatal motoneuron disease with a lifetime risk of 1:800. It is characterized by progressive weakness, muscle wasting and death ensuing 3–5 years after diagnosis (Mitchell and Borasio, 2007). Currently, the only available treatment option is riluzole that prolongs life by 2–3 months, with questionable functional improvement (Miller *et al.*, 2007). The causes of sporadic ALS are unknown but several genes have been identified that pose a genetic risk of developing ALS (Dunckley *et al.*, 2007). In contrast, a number of genes have been identified that, when mutated, cause familial ALS. The best studied of those are mutations in the gene encoding superoxide dismutase 1 (SOD1), responsible for about 2% of all ALS cases.

A number of drug candidates have been proposed but failed in clinical trials. Several reasons have been put forward for this failure, including inability to pass the blood–brain barrier, intolerable side effects and insufficient dosing. Since the exact disease-causing mechanism(s) is unclear at present, a rational approach is to give general trophic support to motoneurons, e.g. by growth factors.

We have recently uncovered the neuroprotective and regenerative properties of the haematopoietic growth factor, granulocyte-colony stimulating factor (G-CSF) (Schneider *et al.*, 2005; Schabitz *et al.*, 2008). Receptors for this factor are present in different brain regions with predominantly neuronal localization (Schneider *et al.*, 2005). G-CSF improves outcome in various stroke models, both with regard to infarct size (Schneider *et al.*, 2005, 2006) and long-term functional recovery (Gibson *et al.*, 2005; Schneider *et al.*, 2006). Together with EPO and the newly discovered neuronal effects of granulocyte-macrophage colony stimulating factor (Kruger *et al.*, 2007; Schabitz *et al.*, 2008), these proteins form a novel class of neurotrophic factors. G-CSF is a 19.6 kDa protein that also passes the intact blood–brain barrier, allowing for peripheral delivery of this protein for the treatment of neurological conditions (Schneider *et al.*, 2005; Zhao *et al.*, 2007).

A major practical advantage of these factors in the treatment of diseases of the brain is their demonstrated safety profile in the traditional clinical indications. G-CSF is clinically used for chemotherapy-associated neutropaenia and stem cell harvesting. In this study, we show that G-CSF is a novel drug candidate for the treatment of ALS.

Materials and Methods

ALS model

We used mice transgenic for the SOD1(G93A) mutation (Gurney *et al.*, 1994) on a C57BL/6 background (B6.Cg-Tg(SOD1-G93A)1Gur/J strain; Jackson Laboratory, Bar Harbour, ME, USA), harbouring the high copy number of the mutant allele human SOD1. The hemizygous line was maintained by mating transgenic males with C57BL/6 wild-type females. Transgenic females were used in all experiments. Experiments were performed in a total of four sequential, age-matched cohorts with equally distributed siblings to treatment and control groups.

Treatment protocol

G-CSF (filgrastim, AMGEN, Thousand Oaks; 30 µg/kg/day) was delivered continuously via an osmotic, subcutaneously implanted, paravertebrally located minipump (Alzet Minipump, model 2004; ALZET Osmotic Pumps, Cupertino, CA, USA). The solvent or vehicle consisted of 250 mM sorbitol, 0.004% Tween-80 and 10 mM sodium acetate buffer (pH 4). Treatment was initiated in all mice at 11 weeks (77 days) of age, for a total of 8 weeks. The minipump was replaced once after 4 weeks.

Assessment of disease progression

Rotarod performance was assessed weekly using the accelerating mode from 3 to 30 r.p.m. Cutoff time was 470 s. Mean of three testings was recorded. Grip strength measurements were done weekly. Mean of three testings was recorded. Clinical onset of disease was defined as the beginning of paralysis of one limb (hind limb). Onset of disease by quantitative tests was defined as a drop in performance to <80% of the initial value (rotarod and grip strength measurements). Clinical end stage was defined as the inability of the animal to right itself over a period of 30 s. Animals were sacrificed at that point. By rotarod and grip strength analysis, clinical end stage was defined as a drop in performance to <20% of the initial value.

Sciatic nerve axotomy

Wild-type mice were anaesthetized using isofluran/N_2O anaesthesia. The left hind leg was slightly stretched and fixated. After dorsal skin incision, the sciatic nerve was carefully exposed and completely cut through with microscissors, 5 mm proximal to the bifurcation of the tibial and common peroneal nerve. ALZET minipumps were implanted as above. After 4 weeks, animals were sacrificed and muscles subjected to histology.

Polymerase chain reaction analysis of differentiated NSC34 cells

NSC34 cells were obtained from Dr Neil Cashman (University of Toronto, Ontario, Canada). Cells were cultured in 15 cm plates with high-glucose Dulbecco modified Eagle medium + 10% foetal calf serum + 1% penicillin/streptomycin + 1% L-glutamine, then split onto 10 cm plates at a density of 3×10^6 cells/plate and differentiated after a minimum of 3 days *in vitro* in high-glucose Dulbecco modified Eagle medium/Ham's F-12 (1:1) (Invitrogen) + 1% foetal calf serum + 1% non-essential amino acids + 1% penicillin/streptomycin + 1% L-glutamine. Cells were scraped off a 10 cm plate in solution D + (4 M guanidine thiocyanate, 25 mM sodium citrate, 0.5% sarkosyl, 0.1 M mercaptoethanol) and RNA extracted by acid phenol–chloroform extraction followed by RNeasy columns (Qiagen, Hilden, Germany). Complementary DNA was synthesized using superscript II reverse transcriptase (Invitrogen, Karlsruhe, Germany) and standard buffers. Polymerase chain reaction (PCR) was run for 32 cycles with an annealing temperature of 60°C and a measuring temperature of 81°C. The following primer pairs were used: murine G-CSF (G-CSF-790s: GGAGCTCTAAGCTTCTAG ATC; G-CSF-1154as: TAGGGACTTCGTTCCTGTGAG; product length 364 bp) and murine GCSF-R (GCSFR-2582s: TGTGCCCCA ACCTCCAAACCA; GCSFR-2817as: GCTAGGGGCCAGAGACAG AGACAC; product length 235 bp). Negative controls did not contain target DNA.

Quantitative reverse transcription–polymerase chain reaction

RNA was isolated from spinal cords using the acidic phenol extraction method followed by purification with the RNeasy Mini Kit (Qiagen), according to the manufacturer's recommendations. Complementary DNA was synthesized from 1 µg total RNA using oligo-dT primers and superscript II reverse transcriptase (Invitrogen), according to standard protocols. Quantitative reverse transcription–polymerase chain reaction (RT–PCR) was performed using the Lightcycler system (Roche) with SYBR-Green staining of double-stranded DNA. Cycling conditions were as follows: 10 min at 95°C; 5 s at 95°C, 10 s at the respective annealing temperature, 30 s at 72°C for 50 cycles and 10 min at 95°C. The following primer pairs were used (annealing and SYBR-Green measuring temperature in parentheses): G-CSF ['G-CSF-790s': GGA GCT CTA AGC TTC TAG ATC; 'G-CSF-1154as': TAG GGA CTT CGT TCC TGT GAG (64°C, 81°C)], G-CSF receptor ['G-CSFR-2582s': TGT GCC CCA ACC TCC AAA CCA; 'G-CSFR-2817as': GCT AGG GGC CAG AGA CAG AGA CAC (64°C, 81°C)], NSE ['mm NSE-p': GGC AAG GAT GCC ACT AAC GT; 'mm NSE-m':

AGG ATC AGC GGG AGA CTT GA (60°C, 84°C)], PLP ['rat PLP-518s': TCA TTC TTT GGA GCG GGT GTG; 'mm PLP-927as': TAA GGA CGG CGA AGT TGT AAG TGG (60°C, 85°C)], GFAP ['mm GFAP-p': CCC AGC TGG TTA GAA TTG GA; 'mm GFAP-m': GGC TAG AGA GAC TTT GCC TC (60°C, 82°C)], IBA1 ['mm iba-1 172s': TGT GGA AGT GAT GCC TGG GA; 'mm iba-1 419as': GGG ATC ATC GAG GAA TTG CTT (60°C, 85°C)], THY1 ['murine thy-1 1167 sense': ACA CAA GCG CTC TGC CAT CAC TG; 'murine thy-1 1477 antisense': GAG GGG CAA GGG AAA GAA GAA TAA (60°C, 84°C)], Bcl-Xl ['Mm Bcl-xL sense': CAG TTT GGA TGC GCG GGA GGT AAT; 'Mm Bcl-xL antisense': AGT GCC CCG CCA AAG GAG AAA AAG (64°C, 85°C)]. Specificity of product was ensured by melting curve analysis and agarose gel electrophoresis. Relative regulation levels were derived after normalization to cyclophilin ['cyc5': ACC CCA CCG TGT TCT TCG AC; 'acyc300': CAT TTG CCA TGG ACA AGA TG (60°C, 82°C)].

SOD1 levels

Analyses were performed on spinal cords of SOD1 transgenic mice receiving G-CSF or vehicle at week 19. To determine SOD1 levels on the mRNA level, quantitative PCR was performed using the following primers: mouse SOD1 'Mm SOD1': sense, GGG TTC CAC GTC CAT CAG TAT GG; antisense, GGC TCC CAG CAT TTC CAG TCT TTG; product length 297 bp. Human SOD1 'Hum SOD1': sense, GTG GGG AAG CAT TAA AGG ACT GAC; antisense, CAA TTA CAC CAC AAG CCA AAC GAC; product length 355 bp. Protein levels were determined by Western blot using antibodies against human SOD (Calbiochem) or mouse SOD1 (Chemicon). Actin (anti-mouse-actin; Chemicon) was used as internal standard. Western blots were quantified using Image J.

Caspase activity assays

For Caspase 3/7 assays, we used the mouse neuroblastoma-motoneuron fusion cell line NSC34. Cells were differentiated as described earlier. Differentiated cells were seeded into 96-well plates (2×10^4 cells/well) for 2 days. To elicit programmed cell death cells were treated with 1 µM staurosporine (Merck-Calbiochem) for 5 h with or without recombinant human G-CSF (Filgrastim, AMGEN) at a concentration of 50 ng/ml. Incubation was continued for 5 h and Caspase 3/7 activity was determined by the CaspaseGlow assay (Promega) with a luminescence plate reader (Mithras, Berthold technologies). Eight independent data points were generated for each treatment.

Akt phosphorylation enzyme-linked immunosorbent assay

To determine possible activation of Akt kinase in NSC34 cells by G-CSF, we utilized the phosphoAkt-Elisa Kit (R&D Systems, Wiesbaden, Germany). NSC34 cells were seeded with differentiation medium into 24-well plates at a density of 8×10^5 cells/well for 3 days. Vehicle or G-CSF was added to a concentration of 50 ng/ml. Treated groups were lysed after 10 or 60 min, the vehicle control at 60 min. The cell lysate was processed according to manufacturer's recommendations. Briefly, the whole lysate was added to the test plate, incubated for 2 h at room temperature and developed with a streptavidin/horseradish peroxidase substrate. Optical densities were measured at 450 and 570 nm (Fluostar, BMG Laboratories, Germany) and pAkt levels were derived from the difference in optical densities and a standard curve and normalized to cell numbers. Absolute values were measured as nanogram per 10^4 cells and converted to relative levels. Four independent data points were obtained for each group.

Immunohistochemistry

After deep anaesthesia, mice were transcardially perfused with Hank's balanced salt solution followed by 4% paraformaldehyde; spinal cords were removed and embedded in paraffin. For G-CSF receptor immunohistochemistry on human spinal cord (tissue kindly provided by Dr J.P. Loeffler, Université Louis Pasteur, Strasbourg, France), sections of paraffin-embedded tissues (10 µm) were deparaffinated and microwaved (citrate buffer at 600 W for 15 min). After overnight incubation of sections at 4°C with the G-CSF receptor antiserum (SC-694; Santa Cruz Biotechnology, Santa Cruz, CA, USA; 1:100), staining was visualized using the ABC technique with 3,3′-diaminobenzidine hydrochloride as chromogen (DAKO). For double-immunofluorescence, sections of paraffin-embedded tissues (10 µm) were deparaffinated and microwaved as described above. Thereafter, sections were incubated at 4°C overnight, simultaneously with the GCSF receptor antiserum (SC-694; Santa Cruz Biotechnology, Santa Cruz, CA, USA; 1:100), the calcitonin gene-related peptide antibody (1720-9007; Biogenesis Ltd, Poole, UK; 1:200), the ChAT antibody (AB144P; Chemicon Europe Ltd, UK; 1:100) or the GFAP antibody (MAB 360; Chemicon Europe Ltd, UK; 1:100). After enhancing the G-CSF receptor staining by adding biotinylated anti-rabbit secondary antibody (Dianova, Hamburg, Germany; 1:200), sections were incubated with streptavidin-coupled fluorophore (Invitrogen, Karlsruhe, Germany; 1:200) or the appropriate fluorescence-coupled secondary antibody (Dianova, Hamburg, Germany; 1:200). The nuclei were counterstained with Hoechst 33342 (Molecular Probes, 1:10 000). Controls included omission of primary antibodies, fluorescence swapping and single-fluorescence stainings.

Stability of G-CSF released from subcutaneously implanted minipumps

Osmotic minipump (Alzet Minipump, model 2004, ALZET Osmotic Pumps, Cupertino, CA, USA) filled with 0.1 µg/µl G-CSF (Filgrastim, AMGEN, Thousand Oaks; 30 µg/kg/day) in 10 mM acetate buffer, pH 4, 250 mM sorbitol and 0.004% Tween-80 were implanted subcutaneously in a paravertebral position in C57BL/6 mice. This results in a release of 30 µg G-CSF/kg body weight over 24 h for a mouse of 20 g weight. The absolute release rate is 0.025 µg G-CSF/h. Serum concentration of G-CSF was determined at days 1, 7 and 28 by enzyme-linked immunosorbent assay (ELISA) (QuantiGlo human G-CSF chemiluminescent ELISA Kit, R&D Systems, Wiesbaden, Germany). The serum was processed according to the manufacturer's recommendations. Briefly, the diluted serum was added to the test plate, incubated for 2 h at room temperature and developed with a luminol/hydrogen phosphate substrate. Chemoluminescence was measured (Luminometer, Berthold, Bad Wildbad, Germany) and G-CSF levels were derived from the difference in the chemoluminescence and standard curve. Five mice were treated for each time point. Measurements were performed in duplicates.

G-CSF levels in the spinal cord after subcutaneous delivery

C57BL/6 mice received G-CSF (filgrastim, AMGEN, Thousand Oaks; 30 µg/kg/day) for 4 days via an osmotic, subcutaneously implanted, paravertebrally located minipump (Alzet Minipump, model 2004, ALZET Osmotic Pumps, Cupertino, CA, USA). Control animals received only vehicle (250 mM sorbitol, 0.004% Tween-80 and 10 mM sodium acetate buffer, pH 4). Spinal cords were dissected after careful transcardial perfusion with Hank's balanced salt solution. Entire spinal cords were homogenized in lysis buffer (Promega) and equal amounts of protein (200 µg) were analysed by an ELISA for human G-CSF (R&D Systems).

Counting of motoneurons

Coronal paraffin sections from the lumbar spinal cord were stained for choline acetyltransferase (CHAT)-positivity using the avidin–biotin complex (ABC) technique with 3,3′-diaminobenzidine hydrochloride as chromogen (DakoCytomation). All neurons in the ventral horn that had a clearly identifiable nucleolus, were >400 µm^2 in size and were CHAT-positive were counted. Eleven sections per mouse spinal cord that were 100 µm apart over a length of 1 mm isolated from the lumbar spinal cord were counted. A total of 14 mice was counted from the vehicle (5), verum (5) and wildtype (4) group.

Counting of muscle fibre diameters

Paraffin sections (10 µm) from indicated muscles (M. quadriceps, M. tibialis) were cut transversally to the length axis of the muscle and stained with haematoxylin and eosin. Countings were performed using Mercator software (ExploraNova, La Rochelle, France), a stereological toolbox.

Electromyography

Single fibre potentials were measured by inserting a concentric electromyography-needle electrode with an outer diameter of 350 µm (Schuler Medizintechnik GmbH, Freiburg, Germany) into the right M. gastrocnemius of anaesthetized (Isoflurane/N_2O) mice. Data were recorded with a PowerLab 4/25 system (ADInstruments GmbH, Spechbach, Germany) at a sample rate of 10 000 Hz. To provide low noise with highest electronic amplification factors, a bioamplifier with headstage system (DAM80, World Precision Instruments, Berlin, Germany) was used (settings: 10 000, low filter of 300 Hz and high filter of 3 kHz). External electromagnetic influence was strongly reduced by a customized Faraday cage (iron mesh with 1 mm wire diameter and open mesh size of 1 cm × 1 cm) and an electrically grounded steel base plate.

Generation of G-CSF overexpressing mice

We cloned the complementary DNA for murine G-CSF in a bidirectional Tet-transactivator responsive vector (pBI, Clontech). EYFP was inserted on the other side of the promoter for easy visualization of expression. To generate the pBI-EYFP-G-CSF ('pBEG') plasmid, G-CSF was amplified from a mouse brain complementary DNA library and inserted into the pBI Tet Vector (Clontech) with NheI and EcoRV, EYFP was inserted into the multiple cloning site I of the vector. Transgenic mice ('BEG') were generated and selected for copy number integration. Copy numbers were estimated by quantitative PCR on genomic DNA by comparing pBEG/cyclophilin ratios of wt and founder mice. The following primer sets were used: pBI-ABG_3947s (GCT GTT GAG ATC CAG TTC GA), pBI-ABG_4788as (AGT CGA CCT AGT TCT AGA GG), cyc5 (ACC CCA CCG TGT TCT TCG AC), acyc300 (CAT TTG CCA TGG ACA AGA TG). Amplification conditions were 60°C annealing and 81°C measuring temperature for the cyclophilin product, and 62°C annealing and 91°C measuring temperature for the pBI-ABG product. Mice of the line BEG6 were crossed with mice expressing the Tet-transactivator (tta) under control of the Thy1-promoter (Thy1-tta) and successful activation of the construct was verified by EYFP imaging.

Statistics

Experiments were performed in a randomized and blinded manner, including computer-generated probe randomizations and probe labelling, blindness of all experimenters to treatment identities until the end of the experiment and separation of data analyses from experiment conduction. Animals were age- and litter matched. Group or pairwise parametric or non-parametric comparisons were done using NCSS software (NCSS, Kaysville, UT, USA). Survival and onset data were analysed using log-rank test. Area under the curve was determined using the trapezoidal algorithm. P-value <0.05 was considered significant. All animal experiments were approved by the appropriate authorities (Regierungspräsidium Karlsruhe, Germany).

Results

The G-CSF receptor is expressed on motoneurons and G-CSF protects against apoptotic cell death

The G-CSF receptor (G-CSFR) is predominantly neuronally expressed in the brain (Schneider *et al.*, 2005). When studying G-CSF receptor expression in the mouse spinal cord, we noted strong expression in the large motoneurons in the ventral horn identified by either calcitonin gene-related peptide or CHAT expression (Fig. 1A and B). Neuronal expression was also confirmed by counterstaining with the astroglial marker GFAP (Fig. 1C and D). G-CSF receptor expression in motoneurons was also confirmed in rat (data not shown) and human (Fig. 2A–C). This motoneuronal expression pattern was also preserved in an ALS patient (Fig. 2D–F) and the SOD1(G93A) mouse model (SupplementaryFig. S1). These expression data suggest that G-CSF may have protective potential in motor neuron diseases such as ALS.

To address the function of G-CSF in motoneurons, we used the well-established murine motoneuron fusion cell line NSC34 (Cashman *et al.*, 1992) that has key characteristics of motoneurons and intact cell death mechanisms that are of relevance to ALS pathophysiology (Oosthuyse *et al.*, 2001; Fukada *et al.*, 2004; Kirby *et al.*, 2005). Differentiated NSC34 cells express both the G-CSF receptor and G-CSF (Supplementary Fig. S2). Addition of G-CSF to the medium leads to activation of Akt kinase,

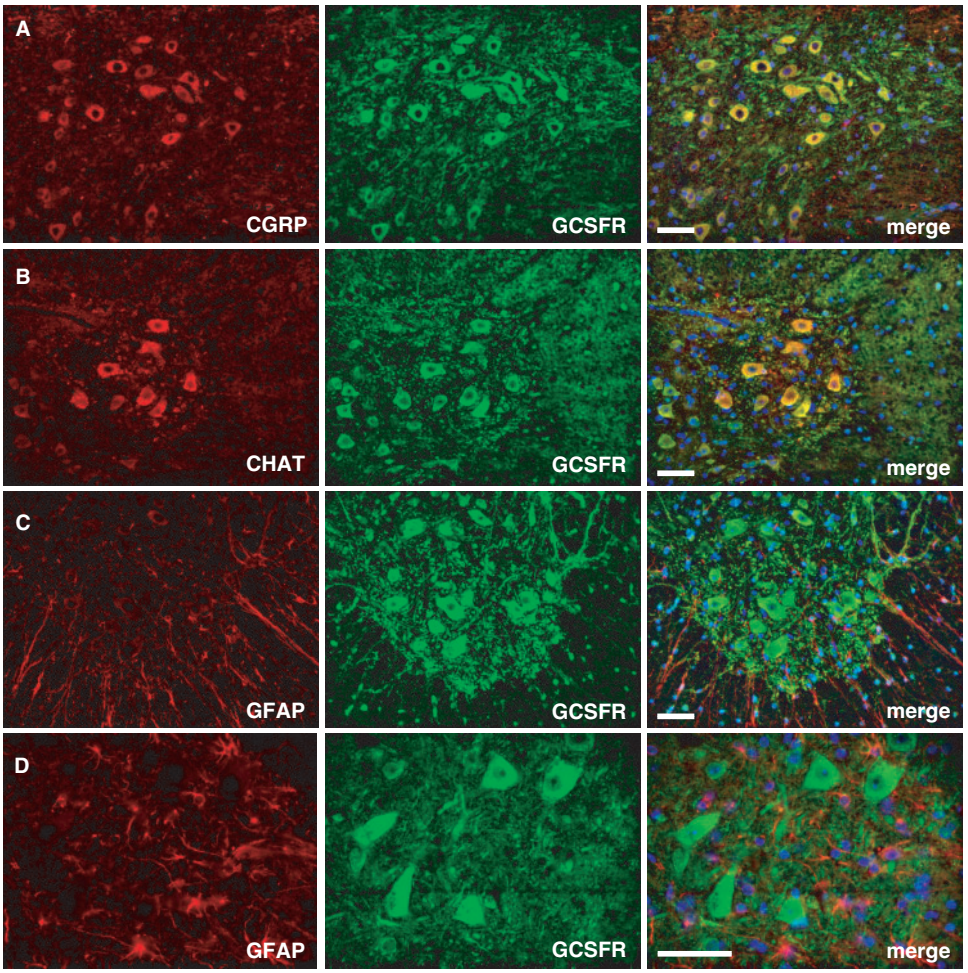

Fig. 1 G-CSFR is expressed on motoneurons in the spinal cord of wt mice. (**A–D**), Immunohistochemistry shows expression of the receptor on large motoneurons in the spinal cord. Double immunfluorescence of G-CSFR and CGRP (calcitonin gene-related peptide) or CHAT (choline acetyltransferase) in the mouse spinal cord ventral horn. CGRP and CHAT are used as marker for motoneurons. Double immunfluorescence of G-CSFR and GFAP revealed the absence of G-CSFR in astrocytes. (**A–C**: × 20 original magnification; all size bars 50 μm; **D**: × 40 original magnification, size bar 25 μm).

determined by its phosphorylation (Fig. 3A). G-CSF strongly reduced caspase-3 activation elicited by the broad-spectrum apoptosis inducer, staurosporin (Fig. 3B). This protective activity of G-CSF in NSC34 cells is supported by data showing protection against H_2O_2-induced cell death (Tanaka *et al.*, 2006).

Subcutaneous delivery of G-CSF improves functional motor performance in the SOD1(G93A)tg mouse model

The most valuable model for ALS are mice transgenic for human mutations in the SOD1 gene, responsible for about 20% of the familial ALS cases (Bendotti and Carri, 2004; Bruijn *et al.*, 2004). For all further analyses we employed the high copy number SOD1(G93A)-transgenic mouse model (Gurney *et al.*, 1994) on a pure C57BL/6 background (Heiman-Patterson *et al.*, 2005) as these mice exhibit a highly stable phenotype and display no gender differences in disease progression (Heiman-Patterson *et al.*, 2005). We detected G-CSF receptor and G-CSF upregulation in SOD1-tg mice that were at a progressed stage of disease (week 19) as an indication of possible relevance of the G-CSF system in this mouse model (>5-fold upregulation of the G-CSF receptor; Fig. 3C).

Consequently, we sought to evaluate effects of systemic G-CSF treatment in this ALS model. Our choice of a treatment regimen was partially guided by our experience in ischemic models where we find efficacy with a one-dose treatment of 60 μg/kg bodyweight (Schabitz *et al.*, 2003; Schneider *et al.*, 2005, 2006) and in the MPTP model where a daily dose of 40 μg/kg bodyweight showed protective effects (Meuer *et al.*, 2006). G-CSF has a moderate plasma half-life of about 4 h in humans and rodents and a number of neurotrophic factors have likely failed in ALS due to short half-lives and low steady-state levels (Apfel, 2001). Under the assumption of a neuroprotective effect on motoneurons in a continuously progressing disease course,

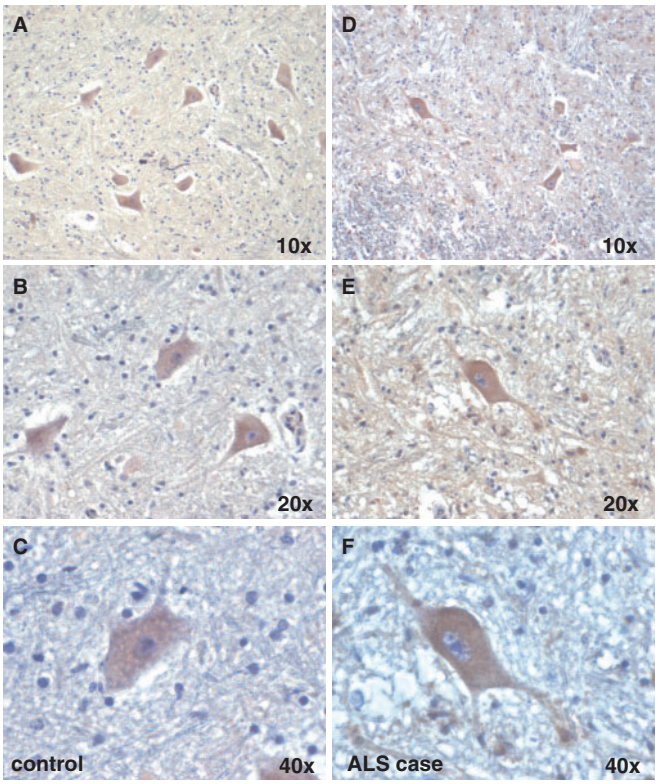

Fig. 2 The G-CSF receptor is expressed on motoneurons in humans. (**A–C**) Immunohistochemical stainings from the ventral horn of the spinal cord of a control patient. (**D–F**) Stainings from an ALS patient (original magnifications from × 10–40 are indicated).

we applied a constant dose of 30 μg/kg bodyweight/day via subcutaneously implanted osmotic minipumps for a total of 8 weeks, starting with week 11. At 11 weeks, SOD1-tg mice did not display overt signs of the disease but already showed muscle fibrillations as early manifestation of the disease (Supplementary Fig. S4). G-CSF was stably secreted under these conditions for the 4 week period until pumps were exchanged (Supplementary Fig. S3). Peripherally applied G-CSF passes the intact blood–brain barrier (Schneider *et al.*, 2005; Zhao *et al.*, 2007). Human G-CSF released by subcutaneous pumps for 4 days in C57BL/6 mice also could be detected at a concentration of 4.2 pg G-CSF/mg spinal cord protein (Supplementary Fig. S5). G-CSF treatment did not alter expression of the endogenous or the transgenic SOD1 mRNA or protein when examined at the end of treatment (week 19; Supplementary Fig. S6).

G-CSF induces expression of anti-apoptotic Bcl-protein in neurons (Schneider *et al.*, 2005). We asked whether we could detect induction of Bcl-Xl in the spinal cord of SOD1-transgenic mice under treatment with G-CSF. Indeed, G-CSF treatment led to induction of Bcl-Xl mRNA compared with SOD1-transgenic treated with vehicle (Fig. 3D), as an indication of anti-apoptotic activity of G-CSF in the spinal cord of SOD1-transgenic mice.

Vehicle-treated SOD1-tg mice progressively declined in their rotarod performance with a strictly linear slope. G-CSF treatment led to a flattening of disease progression with clear separation of the curves after 2–3 weeks of treatment (Fig. 4A). This difference was significant both by analysis of means per timepoint and by analysis of individual areas under the curve. A similar difference was observed for grip strength (measured in mN; Fig. 4B). The difference in the mean areas under the curve is around 40% by both analyses. When looking at the time needed to reach a 50% decline in rotarod performance from week 11, there was a clear delay by >3 weeks in the G-CSF-treated group until the half-maximal decline in performance was reached (Fig. 4C).

G-CSF treatment counteracts muscle atrophy in mutant mice

The major output pathway of ALS, defining its name, is the inability of dying motoneurons, despite enlargement of motor units, to give trophic support to dependent myofibers. This denervation atrophy is typically more patchy in contrast to peripheral nerve lesions due to the stochastic nature of neuronal cell death. We asked whether we could detect any correlate to the strongly improved motor performance in hind limb skeletal muscle histology. When measuring intrafascial diameters of the M. rectus femoris of the quadriceps group at 15 weeks of age (after 4 weeks of treatment), we detected strong muscular atrophy in the vehicle-treated SOD1-tg mice in comparison to wt littermates. In contrast, the G-CSF-treated group had significantly larger muscle diameters (55% increase in diameter, Fig. 4D). In individual muscle fibres, we noted a significant decrease in muscle fibre cross-sectional area in the SOD1-tg animals, which was improved by G-CSF treatment (Fig. 4E). Thus, the increase in functional motor outcome is reflected in muscle morphology.

Occurrence of spontaneous discharges of skeletal muscle fibres ('fibrillations') is one characteristic hallmark of denervation and can be studied by needle electromyography. At week 14, when rotarod performance separates in the two treatment groups, the occurrence of fibrillations is significantly decreased under G-CSF treatment (Fig. 4F and G).

Motor effects of G-CSF are caused by increased survival of motoneurons

Because of the strong effects on muscle phenotype and myotrophic properties of another motoneuron growth factor, IGF-1 (Coleman *et al.*, 1995; Shavlakadze *et al.*, 2005), we explored the possibility of a direct trophic effect of G-CSF on skeletal muscle fibres. We studied chronic denervation caused by unilateral sciatic nerve dissection. Analysis of cross-sectional areas of the M. tibialis anterior 4 weeks after denervation indicated the expected decrease in muscle diameter on the lesion side but G-CSF did not increase the median diameter on the lesioned or the unlesioned side (Supplementary Fig. S7). Therefore, the

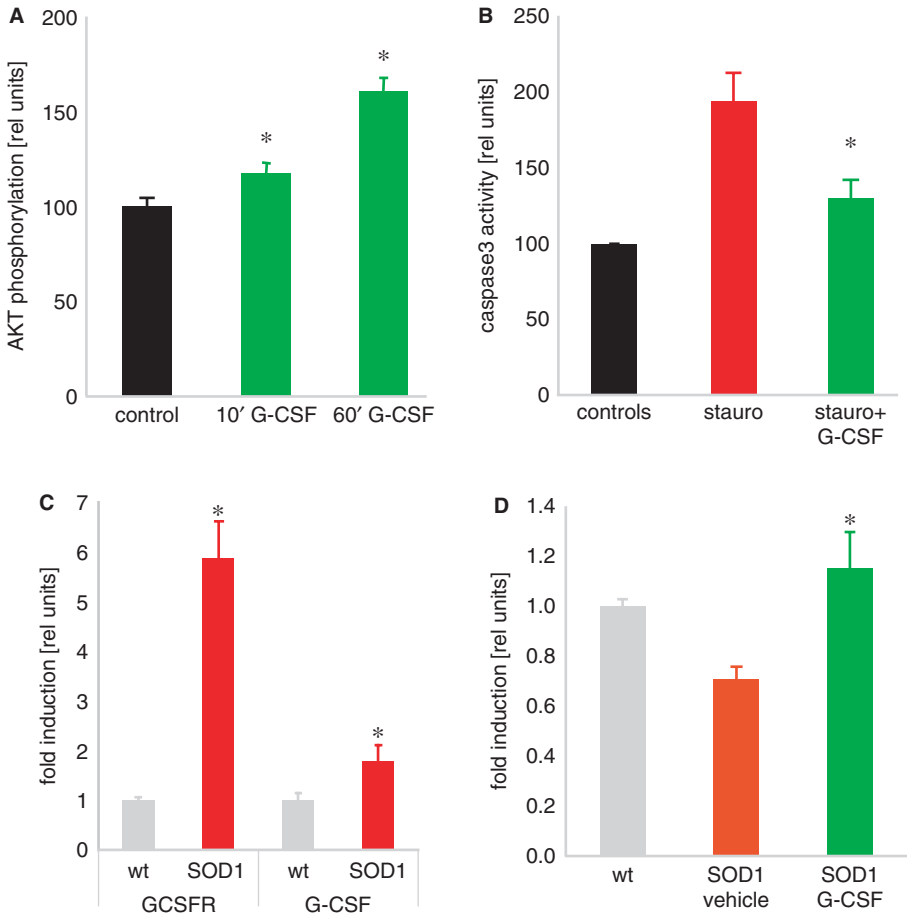

Fig. 3 G-CSF diminishes caspase-activation in a motoneuron cell line, is upregulated together with its receptor in SOD1(G93A) transgenic mice. Treatment with G-CSF induces Bcl-Xl expression in the spinal cord of SOD1 mice. (**A**) G-CSF activates the PI3K-Akt pathway, as demonstrated by an ELISA for phosphorylated Akt ($n = 4$ per treatment, $P < 0.05$). (**B**) Staurosporin-elicited caspase3 activation is diminished by concomitant G-CSF addition ($n = 4$ per treatment, $P < 0.05$). (**C**) G-CSF receptor (G-CSFR) and G-CSF are upregulated in SOD1-tg mice. Quantitative PCR on wt and SOD1-tg mice at 19 weeks of age ($n = 6$–7; $^{*}P < 0.05$). (**D**) Bcl-Xl is upregulated by G-CSF treatment in SOD1-tg mice at 19 weeks of age ($n = 6$–7; $^{*}P < 0.05$).

effect seen in the SOD1(G93A) model is most probably caused by direct actions of G-CSF on motoneurons.

We therefore determined numbers and size distribution of α-motoneurons in the lumbar spinal cord of the SOD-1 tg mice at 15 weeks of age that were defined as (i) being situated in the ventral horn; (ii) having a clearly identifiable nucleolus; (iii) having a minimum cross-sectional area of 400 μm^2 and (iv) staining positive for CHAT. This combination of criteria was chosen to guarantee identification of alpha motoneurons with high specificity (Weber *et al.*, 1997), which are critical for disease progression [e.g. in contrast to γ motoneurons, see Mohajeri *et al.*, (1998)]. We also noted motoneurons with strong or weak CHAT expression. As expected, motoneuron numbers were significantly decreased in the SOD1(G93A) mutant mice as compared with wt mice. This loss was ameliorated by G-CSF treatment (Fig. 5A and B). This beneficial effect was relatively stronger in the population of neurons displaying strong CHAT reactivity, presumably those with higher activity or larger motor fields. Regarding size distribution, we noted that the SOD1(G93A) transgene, in addition to a loss in motoneuron numbers, led to a remarkable downward shift in the remaining motoneuron size, likely due to a more selective demise of larger motoneurons or shrinkage of already damaged motoneurons (Fig. 5B and C).

We also surveyed possible effects of G-CSF on glial cell types in the spinal cord by quantitative PCR. We observed an expected strong increase in mRNA for microglial (IBA1) and astroglial (GFAP) markers in the ALS model, which was not significantly altered by G-CSF treatment (Fig. 5D). Immunohistochemistry revealed predominant localization of these cells in the ventral horn of the spinal cord (data not shown). The pan-neuronal marker NSE was significantly downregulated in the SOD1 model and there was a trend towards higher NSE signals with G-CSF treatment. A significant improvement by G-CSF treatment was noted on the decrease of the oligodendroglial marker PLP in SOD1-tg mice, possibly relating to expression of the G-CSF receptor on oligodendrocytes (Schneider *et al.*, 2005).

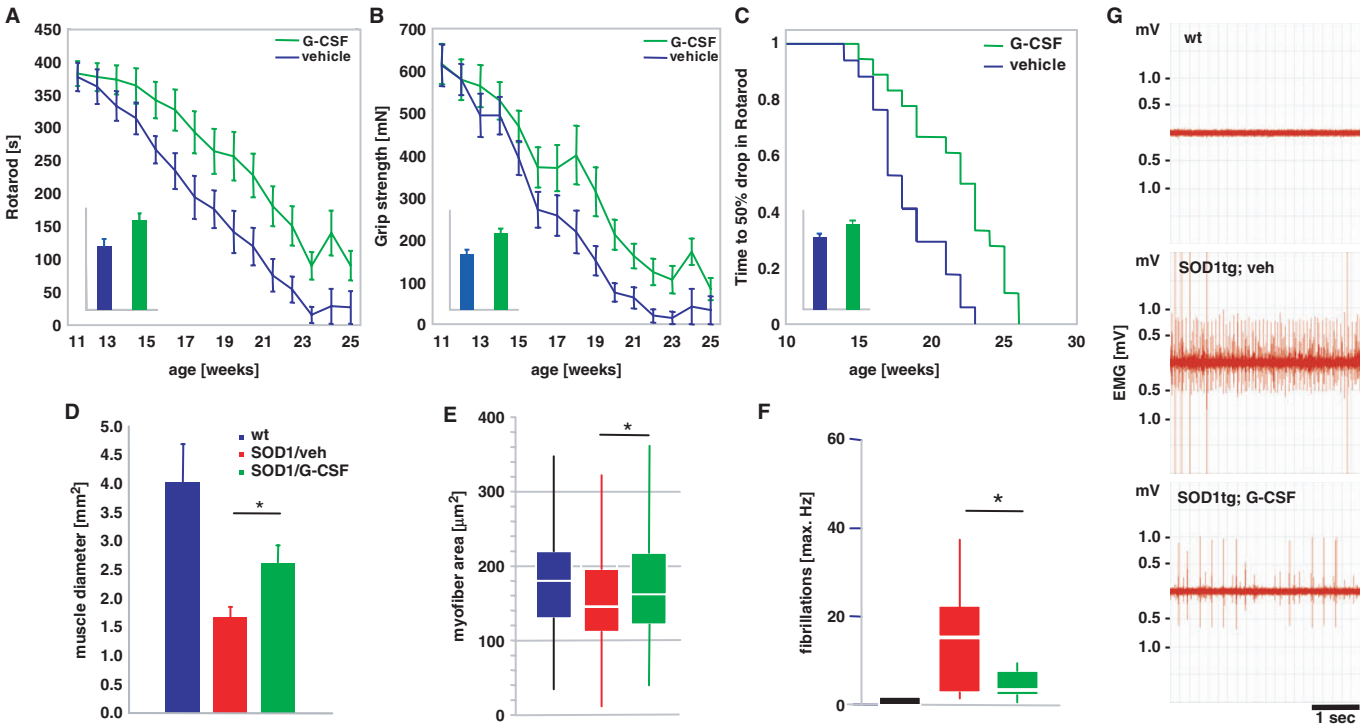

Fig. 4 G-CSF improves motor function in SOD1-tg mice. SOD1 transgenic mice were treated with subcutaneous G-CSF (30 µg/kg/day) or vehicle (vehicle, $n = 17$; G-CSF, $n = 18$) starting at week 11 of age, where signs of muscle denervation are already obvious on EMG. The drugs were continuously administered for 8 weeks with an osmotic minipump (Alzet 2004) that was implanted in a paravertebral position at 11 weeks of age and exchanged at week 15. (**A**) Rotarod performance. Graph depicts means ± SEM over 14 weeks. Inset: AUC, bar graph depicts area under the curve analysis of the individual performance curves. **(B)** Grip strength. Graph depicts means ± SEM over 14 weeks (mN). Inset: AUC, bar graph depicts area under the curve analysis of the individual performance curves. There is considerable improvement in both motor parameters in the treated group (~40% by AUC analysis; $P < 0.05$). (**C**) Kaplan–Meier analysis of the time passed until rotarod performance dropped below 50% of the initial value. Inset: AUC analysis. There is a significant difference between vehicle and G-CSF treatment in all parameters shown (log-rank test; $P < 0.05$). (**D–G**) G-CSF diminishes denervation atrophy in hind limb muscles of SOD1-tg mice. Shown are (**D**) the diameter of the M. rectus femoris of the M. quadriceps group in wt, vehicle-treated and G-CSF-treated SOD1-tg mice. There is a significant increase in the muscle diameter by G-CSF treatment. (**E**) Analysis of individual fibre diameters in the quadriceps group. There is a significant increase in fibre diameter by G-CSF treatment compared with the vehicle-treated group. Shown is a box-blot with median (white) and the 25% and 75% quartiles as box. (**F** and **G**) Quantification of single fiber potentials by electromyography of the M. gastrocnemius in wt, vehicle- and G-CSF-treated SOD1-tg mice at week 14. There is a significant decrease in fibrillations by G-CSF treatment. (**F**) Maximal frequency of fibrillation. (**G**) Exemplary traces from the wt, vehicle- and G-CSF-treated SOD1-tg mice at week 14 ($^*P < 0.05$).

In conclusion, G-CSF improves motoneuron survival and the functional integrity of these neurons, indicated by reduced denervation atrophy, reduced fibrillations and relative preservation of motoneuron size distribution and of choline-acetyltransferase expression.

G-CSF treatment delays onset and prolongs survival in the SOD1(G93A)tg mouse

We compared timed parameters from the vehicle- and G-CSF-treated groups (Fig. 6). Clinically relevant onset of disease as defined by detectable signs of motor deterioration in at least one limb was clearly delayed in the G-CSF-treated group from a mean of 17 weeks to a mean of 18.8 weeks (Fig. 6A). Likewise, when examining the time until rotarod performance dropped below 80% of the initial value at week 11 as a more quantifiable parameter of initial significant motor deterioration, we noted an increase by G-CSF treatment from a mean of 15.2–19.2 weeks (Fig. 6B). This was also paralleled by analysis of grip strength data (not shown). Clinical end stage of disease, defined as inability of the mouse to right itself within 30 s, was also significantly delayed by G-CSF treatment from 21.7 to 23.2 weeks (Fig. 6C). This was again paralleled by looking at time of rotarod decrease below 80% of the initial value (Fig. 6D) and by grip strength analysis. Table 1 summarizes the timed data obtained.

Thus, G-CSF treatment delays onset and prolongs survival in the SOD1 mouse model for ALS.

CNS-targeted overexpression of G-CSF is sufficient to improve outcome

Finally, we chose an alternative approach to increase G-CSF levels in the CNS. We generated transgenic mice harbouring a bidirectional tta-reponsive construct with expression

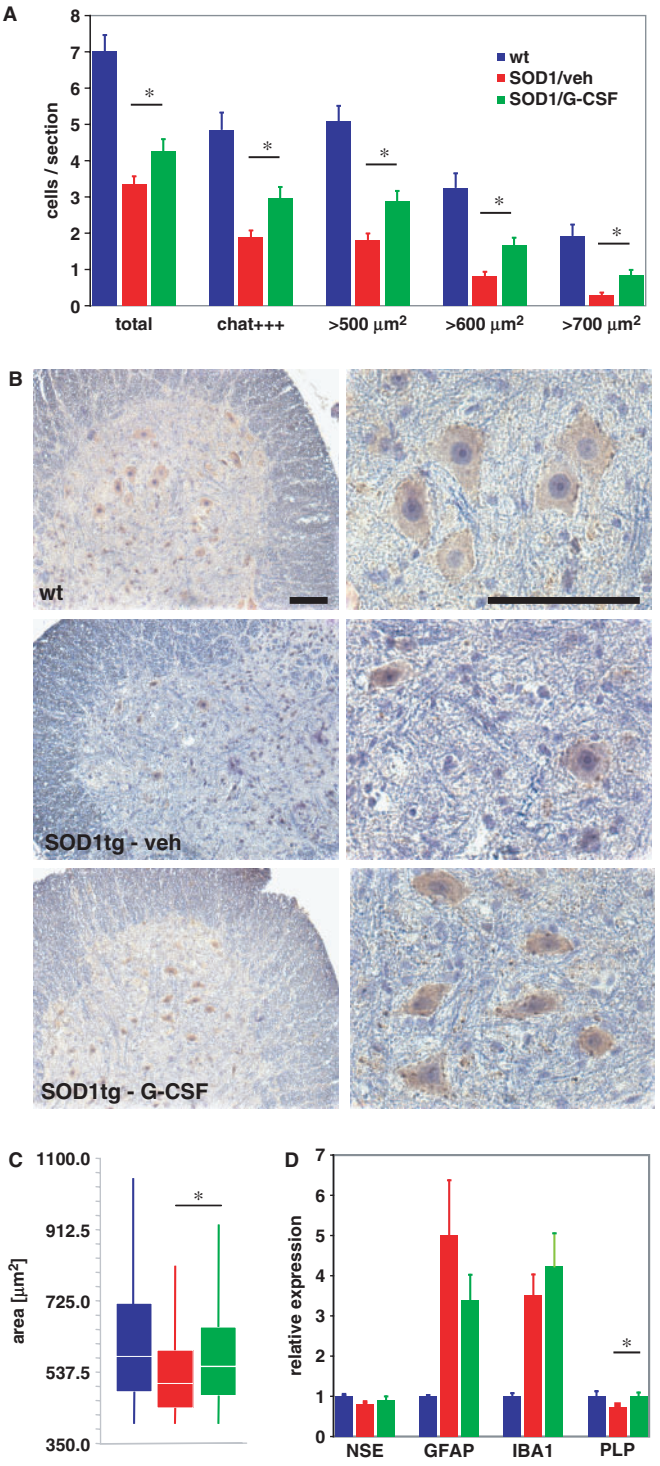

Fig. 5 G-CSF improves motoneuron survival in SOD1-tg mice. (**A**) Quantification of surviving motoneurons in wt, vehicle-treated and G-CSF-treated SOD-1tg mice at 15 weeks of age. We counted 11 sections per mouse spinal cord, 100 μm apart, over a length of 1 mm isolated from the lumbar spinal cord. A total of 14 mice were counted from the vehicle (5), verum (5) and wt (4) groups. There is an increase in motoneurons by G-CSF treatment compared with vehicle, particularly in strongly CHAT-positive and larger motoneurons. (**B**) Examples of the histological evaluation of CHAT-positive cells in the ventral horn of the lumbar spinal cord of 15 weeks wt and SOD-1tg mice treated with either vehicle or G-CSF. Left, ×10 original magnification; right: ×40 original magnification; size bar 100 μm. (**C**) Morphometric evaluation of the size distribution of surviving motoneurons at 15 weeks of age. There is an upward shift in median size distribution by G-CSF treatment (ANOVA on ranks; $P < 0.05$). (**D**) Evaluation of marker expression for different neural cell types by quantitative PCR at week 19. There is no difference in GFAP (astrocytes) or IBA1 (microglia) between vehicle and G-CSF treatment; however, a relative prevention of PLP (oligodendrocyte) decrease in the SOD-tg animals.

cassettes for murine G-CSF and the fluorescent marker EYFP ('pBEG'). These mice were intercrossed with a transgenic tta driver line under control of the Thy1 promoter. Mice harbouring both the pBEG construct and the Thy1-tta driver construct showed strong coexpression of the marker EYFP in cortex layers II and V (Fig. 7A) and strongly elevated levels of G-CSF protein in the brain and spinal cord (Fig. 7B and C). In comparison, littermate controls without the driver construct, but transgenic for the pBEG construct, did not display EYFP expression or elevated G-CSF levels in the CNS (Fig. 7A–C). Heterozygous transgenic mice for pBEG and Thy1-tta were subsequently crossed with SOD1(G93A) transgenic mice and littermates analysed that harboured alleles for both the SOD1(G93A) transgene and the pBEG transgene, with or without the Thy1-tta allele. Presence of the SOD1 transgene did not alter activity of the Thy1-promoter, as evidenced by quantitative PCR analyses of the endogenous Thy1-mRNA (Supplementary Fig. S8A). Mice harbouring the Thy1-tta-driver, the BEG transgene and the SOD1 transgene also demonstrated elevated levels of G-CSF in the spinal cord (Supplementary Fig. S8B). Performance in the rotarod and grip strength tests was significantly improved in mice with the Thy1-tta allele in comparison to littermates without the driver transgene (not shown). When comparing survival, these mice had an increased life expectancy by 10% (Fig. 7D), corroborating our results from the systemic delivery of G-CSF.

Discussion

Therapeutic approaches in ALS

Despite the large international effort invested into ALS research and the undoubtedly great progress that has been made in the field, the basic disease-causing mechanism remains unknown. The genes responsible for several familial ALS forms have been identified and provide novel hints to cellular events that may are involved in ALS pathophysiology. The best-studied mutation and model are SOD1 mutations. However, intense research into the mechanism responsible for the ALS phenotpye of SOD1 mutations has generated a number of novel unexpected questions, most notably on the motoneuron-intrinsic versus a tissue-environmental effect of the mutated SODs (Beers *et al.*, 2006; Boillee *et al.*, 2006; Miller *et al.*, 2006; Nagai *et al.*, 2007).

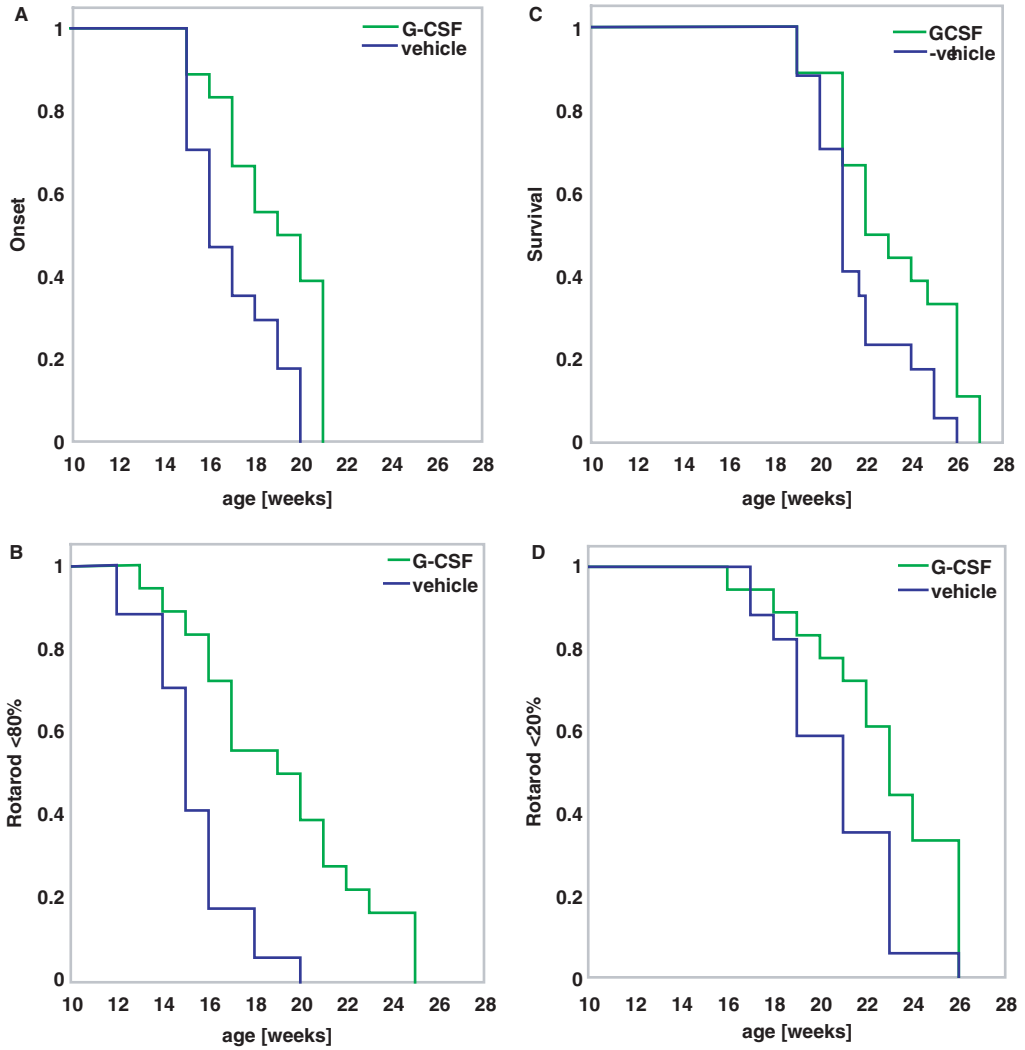

Fig. 6 Timed data for disease onset and endpoint. Kaplan–Meier graphs showing time to disease onset (**A** and **B**) or time to end-stage disease (**C** and **D**). (**A**) Clinical onset of disease defined by detectable signs of motor deterioration in at least one limb. (**B**) Time to drop below 80% of rotarod performance as an objective indicator of initial significant motor deterioration defined as onset. (**C**) Clinical end stage of disease defined as inability of the mouse to right itself within 30 s. (**D**) Time to drop of rotarod performance below 20% as an objective indicator of a significant terminal motor deterioration defined as disease end stage. (log-rank test; $P < 0.05$).

Disease-causing mechanisms that have been proposed include glutamate toxicity, mitochondrial dysfunctions and impaired energy metabolism, oxidative stress and reactive oxygen species, protein aggregation pathology, impaired axonal transport, inflammatory and autoimmune mechanisms and others (McGeer and McGeer, 2005; Carri *et al.*, 2006; Vincent *et al.*, 2008). These hypotheses have led to a large number of trials that have not led to the introduction of novel drugs for ALS patients with the exception of riluzole, a glutamate modifier with modest efficacy. One possible reason for the clinical failure of a large number of drug candidates may be the complexity of the different cell types and mechanisms involved and the use of drug cocktails and combination therapies has been suggested as a remedy (Carri *et al.*, 2006). However, clinical development of combination therapies is problematic.

Table 1 Summary of timed data (weeks) regarding onset, mid-point, and endstage of the disease in the SOD1(G93A)-tg mice treated s.c. with G-CSF

	Vehicle	G-CSF	Difference (%)
Time to clinical onset			
Clinical	17.0	18.8	10.8
Rotarod	15.4	19.2	25.2
Grip Strength	15.0	18.1	20.4
Time to 50% impairment			
Rotarod	18.4	21.6	17.8
Grip strength	17.4	20.1	15.2
Time to endstage			
Clinical	21.7	23.2	7.0
Rotarod	20.8	22.8	10.0
Grip strength	19.5	21.7	11.2

All differences are significant (logrank; $p<0.05$).

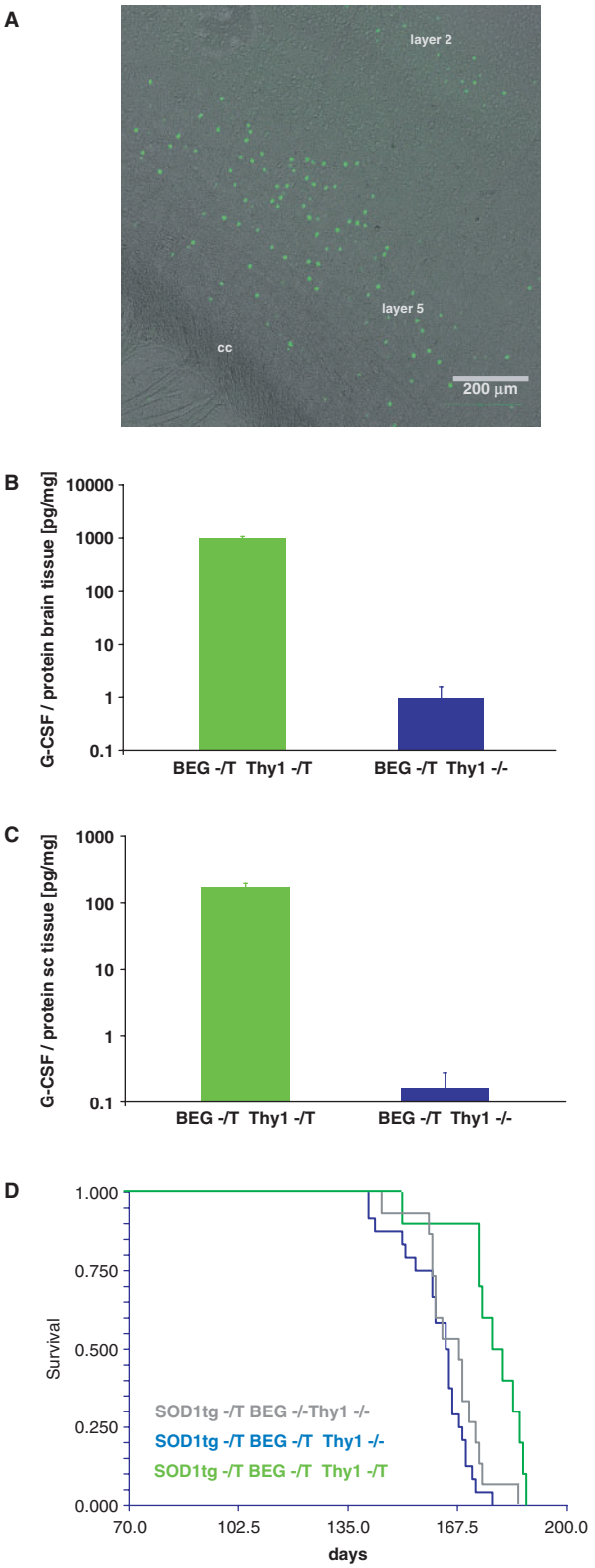

Fig. 7 Survival in SOD1(G93A) transgenic mice crossed with transgenic mice expressing G-CSF in the CNS. (**A**) Double transgenic mice harbouring transgenes for the bidirectional construct BEG (p**B**I; **E**YFP; **G**-CSF) under control of the tta-responsive promotor and a thy1-tta driver express the marker EYFP in the cortex predominantly in layers II and V. Shown is a coronal frontotemporal section of the cortex. (**B** and **C**) Levels of G-CSF protein determined by ELISA in the brains and spinal cords of the double transgenic mice. There is a strong elevation of G-CSF concentration in the CNS of the transgenic mice. (**D**) Survival plot of SOD1(G93A)tg mice crossed with the BEG6 line. The survival analysis includes 24 Thy1-/BEG+/SOD1+, 10 Thy1+/BEG+/SOD1+ and 15 Thy1-/BEG-/SOD1+ mice. Blue lines show the survival in the littermates lacking the Thy1-tta driver that do not overexpress G-CSF in the CNS; green lines, mice that express G-CSF in the CNS. Survival is prolonged by 16.1 days (=10%; Mantel–Haenszel hazard ratio: 5.92; $P < 0.0001$) in the G-CSF overexpressers compared with the Thy1–/BEG+/SOD1+ littermates, and by 11.5 days (=7%; Mantel–Haenszel hazard ratio: 3.99; $P < 0.005$) when compared with Thy1–/BEG–/SOD1+ littermates.

In the absence of an identified singular decisive pathogenic process, providing generic trophic support to motoneurons by growth factors remains a highly rational approach. Currently, two of the most promising candidates for treatment are the proteins IGF1 (Kaspar *et al.*, 2003) and VEGF (Azzouz *et al.*, 2004; Storkebaum *et al.*, 2005). Indeed, one trial with recombinant IGF-1 had a positive outcome (Lai *et al.*, 1997). Here we have shown that the haematopoietic growth factor G-CSF is effective in improving functional parameters and prolonging survival in the SOD1(G93A) mouse model of familial ALS.

Mechanism of action of G-CSF

SOD1 transgenic animals treated with G-CSF demonstrate beneficial effects along the motor pathway: There are more surviving motoneurons in the spinal cord that also appear functionally more intact with larger diameters, electromyographic signs of denervation are reduced, muscle mass is increased and animals show increased strength and endurance and finally, increased survival. The effect of G-CSF is most likely caused by direct protection of motoneurons, as motoneurons in the spinal cord strongly express the receptor for G-CSF, G-CSF is directly protective in a motoneuronal cell line in culture and transgenic overexpression of G-CSF in the CNS improves outcome. At present we have no indication that glial cells might be involved in mediating G-CSF's action: astrocytes and most microglia do not express the receptor and the numbers of these cell types in the SOD1 model are not strongly altered by treatment. It might be possible that immunomodulatory activities of G-CSF also play a role.

We have observed higher PLP mRNA levels in the G-CSF-treated SOD1 transgenic mice. This effect could be indirect or direct. Either there is indeed separate enhancement/rescue of oligodendrocyte function in the SOD1 model or, more likely, the higher PLP expression simply reflects the presence of more surviving motoneurons and thus myelinated axons.

Upregulation of G-CSF in the SOD1-tg model

We see induction of G-CSF and G-CSF receptor in spinal cords of SOD1(G93A) transgenic mice. Upregulation of

G-CSF was also reported by Tanaka *et al.* (2006) in the CSF of ALS patients using an ELISA approach. However, while upregulation of G-CSF receptor was very prominent in the ALS mouse model, Tanaka *et al.* (2006) report downregulation of the receptor in the spinal cord of ALS patients. These data were generated using measurements of optical density of immunoreactivity from light microscopic precipitation stains. This is a methodologically questionable approach and likely not possible without using double-fluorescent staining against an unaltered protein as standard (Schneider *et al.*, 2004). This methodological problem is underlined by the fact that Tanaka *et al.* (2006) could not confirm alterations of G-CSF levels by this approach. We consistently see upregulation of the G-CSF receptor as a reaction to different disease stimuli in the nervous system and believe that this represents an endogenous protective response of neurons (Schneider *et al.*, 2005). We therefore believe that the question of regulation of the G-CSF receptor in ALS patients and possible correlation to the mouse model is open at present.

Predictiveness of the SOD1-tg model

Recently the predictive value of the SOD1-tg model has been questioned mostly because a human trial with the positively tested drug minocycline demonstrated significant worsening of disease progression in the active arm (Gordon *et al.*, 2007). However, the SOD1-tg model remains the only model that reproduces the main features of the human disease. A possible explanation of the discrepancy between successfully tested drugs in the model and failures in the clinical trials is inadequate conduction of preclinical studies (Scott *et al.*, 2008). Our study relied on a fully blinded (both for treatment allocation as well as outcome measures) and randomized design using littermate and age matching. The effects have also been confirmed by a different delivery approach, transgenic overexpression. We are therefore confident that our results represent true effects of G-CSF. Of note, we have also started treatment at a time when SOD1 mice already display clear electromyographic denervation signs.

Effect size

We have observed a total benefit in survival by 7% with systemic delivery of G-CSF (or about 10% by a transgenic approach) and an overall increase in strength and endurance by about 40% during the observation period. It is possible that prolonging treatment beyond the 8 week period could have further increased the survival benefit. The observed effect on survival might appear moderate; it is however very difficult to compare this with other studies in this model due to substantial differences in experimental conditions between the animal studies performed to date (Scott *et al.*, 2008). In general, very large effects on survival have only been obtained by siRNA targeting of the disease-causing protein itself or by viral delivery of proteins. In contrast, the effects observed on motor performance are remarkably strong and it is tempting to speculate that this might translate to longer periods of independence for human patients.

Clinical application of G-CSF

G-CSF may have considerable practical advantages over other discussed growth factors for the treatment of ALS: It has a safe clinical track record in other indications (Hubel and Engert, 2003), is generally well tolerated, passes the intact blood–brain barrier (Schneider *et al.*, 2005; Zhao *et al.*, 2007) and has already entered clinical development in another neurological disorder, stroke (Schabitz and Schneider, 2007). In addition, the pharmacology of G-CSF is extremely well understood. Translation to clinical development of G-CSF in ALS and possibly other motoneuron disorders appears very feasible.

Acknowledgements

The authors acknowledge the excellent technical assistance of Claudia Heuthe, Sandra Ellering, Ulrike Bolz, Frank Herzog and Gisela Eisenhardt. We are indebted to Dr Neil Cashman (University of Toronto, Ontario, Canada) for sharing the NSC34 cell line with us. We thank Dr J.P. Loeffler (Université Louis Pasteur, Strasbourg, France) for the gift of human spinal cord samples.

References

Apfel SC. Neurotrophic factor therapy–prospects and problems. Clin Chem Lab Med 2001; 39: 351–5.

Azzouz M, Ralph GS, Storkebaum E, Walmsley LE, Mitrophanous KA, Kingsman SM, et al. VEGF delivery with retrogradely transported lentivector prolongs survival in a mouse ALS model. Nature 2004; 429: 413–7.

Beers DR, Henkel JS, Xiao Q, Zhao W, Wang J, Yen AA, et al. Wild-type microglia extend survival in PU.1 knockout mice with familial amyotrophic lateral sclerosis. Proc Natl Acad Sci USA 2006; 103: 16021–6.

Bendotti C, Carri MT. Lessons from models of SOD1-linked familial ALS. Trends Mol Med 2004; 10: 393–400.

Boillee S, Yamanaka K, Lobsiger CS, Copeland NG, Jenkins NA, Kassiotis G, et al. Onset and progression in inherited ALS determined by motor neurons and microglia. Science 2006; 312: 1389–92.

Bruijn LI, Miller TM, Cleveland DW. Unraveling the mechanisms involved in motor neuron degeneration in ALS. Annu Rev Neurosci 2004; 27: 723–49.

Carri MT, Grignaschi G, Bendotti C. Targets in ALS: designing multidrug therapies. Trends Pharmacol Sci 2006; 27: 267–73.

Cashman NR, Durham HD, Blusztajn JK, Oda K, Tabira T, Shaw IT, et al. Neuroblastoma x spinal cord (NSC) hybrid cell lines resemble developing motor neurons. Dev Dyn 1992; 194: 209–21.

Coleman ME, DeMayo F, Yin KC, Lee HM, Geske R, Montgomery C, et al. Myogenic vector expression of insulin-like growth factor I stimulates muscle cell differentiation and myofiber hypertrophy in transgenic mice. J Biol Chem 1995; 270: 12109–16.

Dunckley T, Huentelman MJ, Craig DW, Pearson JV, Szelinger S, Joshipura K, et al. Whole-genome analysis of sporadic amyotrophic lateral sclerosis. N Engl J Med 2007; 357: 775–88.

Fukada K, Zhang F, Vien A, Cashman NR, Zhu H. Mitochondrial proteomic analysis of a cell line model of familial amyotrophic lateral sclerosis. Mol Cell Proteomics 2004; 3: 1211–23.

Gibson CL, Bath PM, Murphy SP. G-CSF reduces infarct volume and improves functional outcome after transient focal cerebral ischemia in mice. J Cereb Blood Flow Metab 2005; 25: 431–9.

Gordon PH, Moore DH, Miller RG, Florence JM, Verheijde JL, Doorish C, et al. Efficacy of minocycline in patients with amyotrophic lateral sclerosis: a phase III randomised trial. Lancet Neurol 2007; 6: 1045–53.

Gurney ME, Pu H, Chiu AY, Dal Canto MC, Polchow CY, Alexander DD, et al. Motor neuron degeneration in mice that express a human Cu,Zn superoxide dismutase mutation. Science 1994; 264: 1772–5.

Heiman-Patterson TD, Deitch JS, Blankenhorn EP, Erwin KL, Perreault MJ, Alexander BK, et al. Background and gender effects on survival in the TgN(SOD1-G93A)1Gur mouse model of ALS. J Neurol Sci 2005; 236: 1–7.

Hubel K, Engert A. Clinical applications of granulocyte colony-stimulating factor: an update and summary. Ann Hematol 2003; 82: 207–13.

Kaspar BK, Llado J, Sherkat N, Rothstein JD, Gage FH. Retrograde viral delivery of IGF-1 prolongs survival in a mouse ALS model. Science 2003; 301: 839–42.

Kirby J, Halligan E, Baptista MJ, Allen S, Heath PR, Holden H, et al. Mutant SOD1 alters the motor neuronal transcriptome: implications for familial ALS. Brain 2005; 128: 1686–706.

Kruger C, Laage R, Pitzer C, Schabitz WR, Schneider A. The hematopoietic factor GM-CSF (Granulocyte-macrophage colony-stimulating factor) promotes neuronal differentiation of adult neural stem cells in vitro. BMC Neurosci 2007; 8: 88.

Kruger C, Laage R, Pitzer C, Schabitz WR, Schneider A. The hematopoietic factor GM-CSF (granulocyte-macrophage colony-stimulating factor) promotes neuronal differentiation of adult neural stem cells in vitro. BMC Neurosci 2007b; 8: 88.

Lai EC, Felice KJ, Festoff BW, Gawel MJ, Gelinas DF, Kratz R, et al. Effect of recombinant human insulin-like growth factor-I on progression of ALS. A placebo-controlled study. The North America ALS/IGF-I Study Group. Neurology 1997; 49: 1621–30.

McGeer EG, McGeer PL. Pharmacologic approaches to the treatment of amyotrophic lateral sclerosis. BioDrugs 2005; 19: 31–7.

Meuer K, Pitzer C, Teismann P, Kruger C, Goricke B, Laage R, et al. Granulocyte-colony stimulating factor is neuroprotective in a model of Parkinson's disease. J Neurochem 2006; 97: 675–86.

Miller RG, Mitchell JD, Lyon M, Moore DH. Riluzole for amyotrophic lateral sclerosis (ALS)/motor neuron disease (MND). Cochrane Database Syst Rev 2007: CD001447.

Miller TM, Kim SH, Yamanaka K, Hester M, Umapathi P, Arnson H, et al. Gene transfer demonstrates that muscle is not a primary target for non-cell-autonomous toxicity in familial amyotrophic lateral sclerosis. Proc Natl Acad Sci USA 2006; 103: 19546–51.

Mitchell JD, Borasio GD. Amyotrophic lateral sclerosis. Lancet 2007; 369: 2031–41.

Mohajeri MH, Figlewicz DA, Bohn MC. Selective loss of alpha motoneurons innervating the medial gastrocnemius muscle in a mouse model of amyotrophic lateral sclerosis. Exp Neurol 1998; 150: 329–36.

Nagai M, Re DB, Nagata T, Chalazonitis A, Jessell TM, Wichterle H, et al. Astrocytes expressing ALS-linked mutated SOD1 release factors selectively toxic to motor neurons. Nat Neurosci 2007; 10: 615–22.

Oosthuyse B, Moons L, Storkebaum E, Beck H, Nuyens D, Brusselmans K, et al. Deletion of the hypoxia-response element in the vascular endothelial growth factor promoter causes motor neuron degeneration. Nat Genet 2001; 28: 131–8.

Schabitz WR, Schneider A. New targets for established proteins: exploring G-CSF for the treatment of stroke. Trends Pharmacol Sci 2007; 28: 157–61.

Schabitz WR, Kollmar R, Schwaninger M, Juettler E, Bardutzky J, Scholzke MN, et al. Neuroprotective effect of granulocyte colony-stimulating factor after focal cerebral ischemia. Stroke 2003; 34: 745–51.

Schabitz WR, Kruger C, Pitzer C, Weber D, Laage R, Gassler N, et al. A neuroprotective function for the hematopoietic protein granulocyte-macrophage colony stimulating factor (GM-CSF). J Cereb Blood Flow Metab 2008; 28: 29–43.

Schneider A, Kruger C, Steigleder T, Weber D, Pitzer C, Laage R, et al. The hematopoietic factor G-CSF is a neuronal ligand that counteracts programmed cell death and drives neurogenesis. J Clin Invest 2005; 115: 2083–98.

Schneider A, Laage R, von Ahsen O, Fischer A, Rossner M, Scheek S, et al. Identification of regulated genes during permanent focal cerebral ischaemia: characterization of the protein kinase 9b5/MARKL1/MARK4. J Neurochem 2004; 88: 1114–26.

Schneider A, Wysocki R, Pitzer C, Kruger C, Laage R, Schwab S, et al. An extended window of opportunity for G-CSF treatment in cerebral ischemia. BMC Biol 2006; 4: 36.

Scott S, Kranz JE, Cole J, Lincecum JM, Thompson K, Kelly N, et al. Design, power, and interpretation of studies in the standard murine model of ALS. Amyotroph Lateral Scler 2008; 9: 4–15.

Shavlakadze T, White JD, Davies M, Hoh JF, Grounds MD. Insulin-like growth factor I slows the rate of denervation induced skeletal muscle atrophy. Neuromuscul Disord 2005; 15: 139–46.

Storkebaum E, Lambrechts D, Dewerchin M, Moreno-Murciano MP, Appelmans S, Oh H, et al. Treatment of motoneuron degeneration by intracerebroventricular delivery of VEGF in a rat model of ALS. Nat Neurosci 2005; 8: 85–92.

Tanaka M, Kikuchi H, Ishizu T, Minohara M, Osoegawa M, Motomura K, et al. Intrathecal upregulation of granulocyte colony stimulating factor and its neuroprotective actions on motor neurons in amyotrophic lateral sclerosis. J Neuropathol Exp Neurol 2006; 65: 816–25.

Vincent AM, Sakowski SA, Schuyler A, Feldman EL. Strategic approaches to developing drug treatments for ALS. Drug Discov Today 2008; 13: 67–72.

Weber UJ, Bock T, Buschard K, Pakkenberg B. Total number and size distribution of motor neurons in the spinal cord of normal and EMC-virus infected mice–a stereological study. J Anat 1997; 191 (Pt 3): 347–53.

Zhao LR, Navalitloha Y, Singhal S, Mehta J, Piao CS, Guo WP, et al. Hematopoietic growth factors pass through the blood-brain barrier in intact rats. Exp Neurol 2007; 204: 569–73.